Master's Program in Molecular Medicine
at the Charité - Universitätsmedizin Berlin

Master's Thesis

to earn the

Master of Science in Molecular Medicine

Characterizing the Role of a GLUT1 Mutation in GLUT1-deficiency Syndrome

Presented by

Jingyuan Cheng

Born on May 17th, 1993

First Evaluator: Professor Dr. Matthias Selbach

Second Evaluator: Professor Dr. Volker Haucke

Completed at AG Selbach, Max Delbrück Center for Molecular Medicine

Abstract

Glucose transporter-1 (GLUT1) deficiency syndrome is a genetic disorder characterized by impaired glucose transport into the brain. One of the clinically identified pathogenic mutations is a Pro485-to-Leu substitution located in the cytoplasmic carboxyl tail of GLUT1, whose pathogenic mechanisms remain unclear. A previous *in vitro* proteomic screen from our group revealed that this GLUT1 mutation leads to specific interactions with clathrins, which is supported by the further bioinformatic finding that the mutation creates a novel dileucine motif known to mediate clathrin-dependent trafficking.

In this study we used stable inducible HEK293 cells to further investigate the effect of the GLUT1 mutation on the intracellular localization and trafficking of the protein. We showed that the wild type GLUT1 mainly localizes to the plasma membrane, whereas the mutant GLUT1 mislocalizes to intracellular compartments and co-localizes with endocytosed transferrin, as well as early endosomal and late endosomal markers. Moreover, SILAC-based quantitative characterization of proximate proteins also identified increased proximate interaction of the mutant GLUT1 with proteins associated with endocytosis and endosomal compartments. Together, these data suggest that the GLUT1^{P485L} mutation causes internalization of the GLUT1 protein via clathrin-mediated endocytosis, thus leading to GLUT1 deficiency syndrome.

Contents

List of Figures

Introduction

As the primary glucose transporter across the endothelial cells of the blood-brain barrier, the facilitated glucose transporter member 1 (GLUT1) protein plays a central role in the regulation of brain energy metabolism and maintenance of central nervous system homeostasis [1]. Human GLUT1 is encoded by the *SLC2A1* gene on the short arm of chromosome 1, consists of 492 amino acids and contains 12 transmembrane α helices [2, 3]. GLUT1 is highly expressed in endothelial cells and glial cells, but is ubiquitously expressed at lower levels as well [4, 5]. Two isoforms of GLUT1 have been found, namely the 55kDa form with N-linked glycosylation at Asn45 and the 45kDa unglycosylated form [6, 7].

Mutations in the *SLC2A1* gene can result in GLUT1 deficiency syndrome (G1DS), an autosomal dominant disorder caused by impaired GLUT1-mediated glucose transport into the brain [8, 9]. To date, approximately 80 mutations in the *SLC2A1* gene have been detected in about 140 patients, including large-scale deletions, insertions, missense, nonsense, frame shift, translation initiation and splice-site mutations [10, 11]. These mutations are heterozygous resulting in GLUT1 haploinsufficiency - absence or loss of a functional allele [9, 11]. The classic G1DS phenotype consist of intractable epilepsy presenting in infancy, delayed neurologic development, secondary microcephaly and complex movement disorders [8, 9]. Milder variants have been reported to affect about 10% G1DS patients and present mental retardation, movement abnormalities but without clinical seizures [10, 12]. The diagnostic hallmark of G1DS features reduced cerebrospinal fluid (CSF) glucose concentration (hypoglycorrhachia) combined with low CSF lactate and low 3-O-methyl-D-glucose uptake in erythrocytes [10, 13]. The ketonic diet, introduced as a treatment for G1DS in 1991, provides an alternative fuel for brain metabolism and effectively controls the seizures in G1DS patients [10].

1.1 The GLUT1$^{\mathbf{P485L}}$ mutation

One of the clinically identified missense mutations in GLUT1 is a Pro485-to-Leu substitution (GLUT1$^{\mathrm{P485L}}$) located in the cytoplasmic carboxyl tail [1, 14]. However, the molecular

mechanisms by which the mutation causes the disease remains elusive. In a previous proteomic screen study to investigate the impact of disease-causing mutations, the GLUT1^{P485L} mutation was found to lead to an increased binding of clathrins. Sequence analysis revealed that the mutation creates a dileucine motif known to mediate clathrin-dependent endocytosis ([D/E]XXXL[L/I]) in the cytoplasmic tail [15, 16].

1.2 Clathrin-mediated endocytosis

Based on these findings, it is hypothesized that the GLUT1^{P485L} mutation causes clathrin-mediated endocytosis and possibly subsequent degradation of GLUT1, leading to the development of GLUT1-deficiency syndrome. The hypothesis will be further investigated in this master thesis.

Materials and methods

Cell line generation

Stable cell lines expressing the wildtype and mutant GLUT1 were kindly provided by Katrina Meyer and Markus Landthaler at Max Delbrück Center. In brief, the gene *SLC2A* was purchased from Harvard Plasmid Repository and a stop codon was added with the primers listed in Table 2.1. The P485L mutation was introduced by polymerase chain reaction-directed mutagenesis with the primers in Table 2.1. The wildtype and mutant *SLC2A* coding sequences

TABLE 2.1: Primer sequences for GLUT1 cloning.

Primer	**Sequence from 5' to 3'**
Stop codon forward	TCCCAAGTGTAATTGCCAACTTTCTTGTACAAAGTTG
Stop codon reverse	ATCAGCCCCCAGGGGATG
P485L forward	CTGTTCCATCtCCTGGGGGCT
P485L reverse	CTCCTCGGGTGTCTTGTCAC

were recombined into the vector pDEST-pcDNA5-BirA-FLAG N-term [17] using Gateway cloning system (ThermoFisher), as illustrated in Figure 2.1. Stable HEK293 cell lines were generated using the Flp-In T-REx system. A control 293T-REx cell line was generated in a similar manner wildtypewith an integrated transgene for the inducible expression of GFP1-10.

Cell culture

HEK293 cells were cultured at 37 °C and 5% CO_2 in T-75 flasks (CELLSTAR) at approximately 10% confluency in DMEM (Life Technologies) complemented with 10% fetal bovine serum (Pan-Biotech). The medium is referred to complete DMEM in the following. Cells were routinely passaged twice a week as follows: the medium was aspirated and the cells were briefly washed with 4 mL sterile pre-warmed PBS (Life Technologies). To detach the cells 1 mL trypsin-EDTA (0.05%, Life Technologies) was added and the flask was placed in an incubator at 37 °C and 5% CO_2 for 1 min. Trypsin was then inactivated with 9 mL pre-warmed complete DMEM. The medium was gently pipetted to the bottom of the flask in

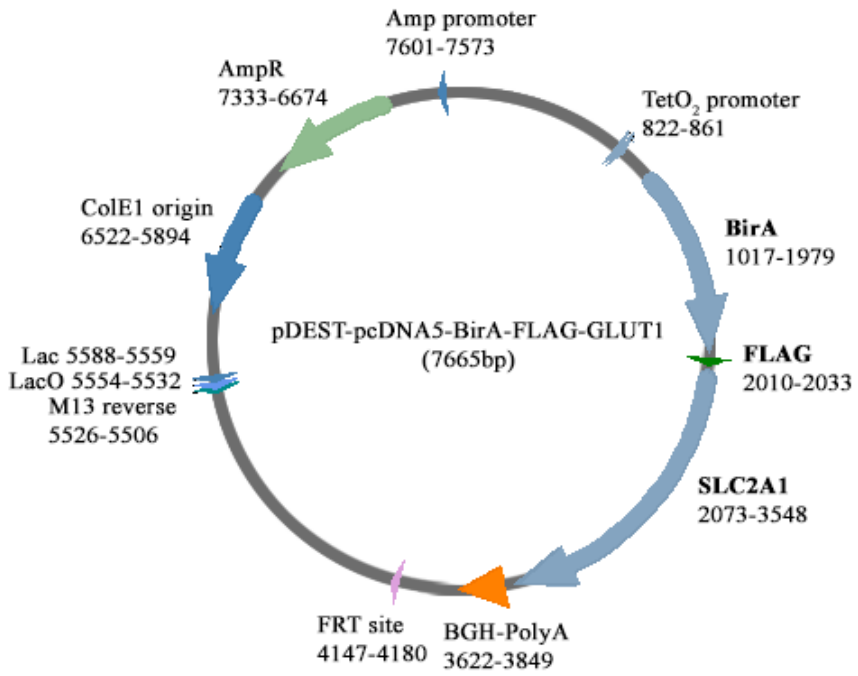

FIGURE 2.1: Graphic maps of the recombinant plasmids.

order to recover all the cells and homogenize them. 1 mL of the cell suspension was transferred into 10 mL fresh warm complete DMEM in a new culture flask which was then placed back in the incubator. The cells would reach approximately 80% confluency before the next passaging.

Cells used for SILAC based experiments were cultured in SILAC DMEM (Life Technologies) complemented with glutamine (Glutamax, Life Technologies), pyruvate (Life Technologies), non-essential amino acids (Life Technologies) and 10% dialyzed fetal bovine serum (Pan-Biotech). In addition, L-arginine (Arg0, Sigma-Aldrich) and L-lysine (Lys0, Sigma-Aldrich) were added to the Light SILAC DMEM to a final concentration of 0.199 mM and 0.339 mM, respectively. Alternatively, Arg6 and Lys4 or Arg10 and Lys8 were added in place of their Light counterparts to make Medium-heavy SILAC DMEM and Heave SILAC DMEM, respectively. PBS-EDTA (Lonza) was used to detach the cells when passaging as trypsin may contain amino acids. After six passages cells were fully labeled as assessed by MS.

For the doxycycline induction experiments unlabeled HEK cells were cultured in 6-well plates. The cells were grown to approximately 50% confluency on the second day after seeding. The medium was removed and 2 mL complete DMEM containing doxycycline (Sigma-Aldrich) was carefully added to each well. After 24 hr or 48 hr the cells were harvested for

western blot analysis.

For the BioID experiments fully labeled HEK293 cells were seeded in 15 cm plates with approximately 25% density. Two plates were used for each condition. HEK293 stable cells expressing GFP1-10 were labeled in Light SILAC DMEM and used as negative control cells. Besides the Light control cells, in the forward experiment mutant GLUT1 cells were cultured in Medium-heavy SILAC DMEM and mutant GLUT1 cells were cultured in Heavy SILAC DMEM, while in the reverse label-swap experiment mutant GLUT1 cells were cultured in Medium-heavy SILAC DMEM and mutant GLUT1 cells were cultured in Heavy SILAC DMEM. The cells were grown to 40%-50% confluency before being treated with 0.1 µg/mL doxycycline and 1 mM biotin (ThermoFisher). After 24 hr, the cells were scraped in ice-cold PBS and spun down at 300 rcf, 4 °C for 4 min. After resuspension in ice-cold PBS, the triple SILAC labels were combined into a forward and a reverse experiment. The cells were spun down again and the cell pellets were collected for further BioID purification and MS analysis.

For the immunofluorescence experiments sterile glass coverslips (Roth, 18 mm diameter, 0.170 mm thickness) were placed in a 12-well plate. Poly-L-lysine (0.01%, Sigma-Aldrich) was added to each well to cover the coverslips. After incubation at room temperature for 5 min, poly-L-lysine was recovered from the wells and stored at 4 °C. The coverslips were washed twice with sterile H_2O before being air-dried completely. HEK293 cells were then counted and seeded in the plate with approximately 25% density. The cells were treated with 0.1 µg/mL doxycycline on the second day and subjected to subsequent immunostaining on the third day.

Western blot

Cells were grown in 6-well plates as described above. After doxycycline or inhibitor treatment, cells were scraped in ice-cold PBS and spun down at 300 rcf, 4 °C for 4 min. Cell pellets were lyzed for 15 min at room temperature in lysis buffer (50 mM ABC solution, 2% SDS, supplemented with 0.5 µL benzonase (Sigma-Aldrich) and 0.2 tablet protease inhibitors (Roche) per 2 mL lysis buffer). Lysates were spun down at 140 000 rpm for 15 min to remove cell debris and supernatants were transferred to new Eppendorf tubes. For each SDS-PAGE sample, 15 µL supernatant was diluted in LDS sample buffer (NOVEX) complemented with 1 µL 1M DTT (Sigma-Aldrich) before being heated at 70 °C for 10 min in a thermoblock. Samples were then loaded onto a 4%-12% gel (NOVEX) along with protein ladders (PageRuler Plus, ThermoFisher). Proteins were separated using electrophoresis for 90 min at 150 V in 400 mL MES running buffer (ThermoFisher).

Before transferring a PVDF membrane (Merck Millipore) was activated in methanol for 1 min and equilibrated in transfer buffer (25 mM Tris-HCl, 190 mM glycine, 20% methanol, pH 8.3) for 10 min. Whatman filter papers and sponges were also soaked in transfer buffer for 10 min. A tank blotting system (Invitrogen) was used to transfer the separated proteins to the membrane. In short, a transfer sandwich was prepared with the membrane on the cathode and the gel on the anode. Air bubbles were remove with a roller between the gel and the membrane. The cassette was then placed in the transfer tank on ice and the proteins were transferred at a constant current of 250 mA for 2 hr.

After transferring the membrane was blocked in 5% milk powder in TBST (150 mM sodium chloride, 20 mM Tris-HCl, 0.1% Tween-20, pH 7.6) at room temperature for 30 min. The membrane was then incubated with the primary antibody diluted in blocking buffer while rotating at 4 °C. The membrane was washed 3 times for 5 min in TBST before being incubated at room temperature for 1 hr with the HRP-conjugated secondary antibody diluted in blocking buffer. The membrane was washed again before the chemiluminescence substrate (PerkinElmer) was applied to the membrane. The chemiluminescent signals were captured using a ChemiDoc MP Imaging System (Bio-Rad) and analyzed with Image Lab software version 5.2.1. The primary and secondary antibodies used in this thesis are summarized in Table 2.2.

TABLE 2.2: Antibodies used for western blot and their dilutions.

Antibodies	**Source**	**Dilution**	**Conjugate**
Rabbit polyclonal anti-FLAG	Cell Signaling Technology	1:1000	HRP
Rabbit polyclonal anti-LC3	Novus Biologicals	1:1000	
Mouse monoclonal anti-β-actin	Sigma-Aldrich	1:10 000	
Anti-rabbit IgG	GE Healthcare	1:10 000	HRP
Anti-mouse IgG	GE Healthcare	1:25 000	HRP

BioID and MS analysis

Cell pellets from 15 cm plates were incubated at 4 °C in 1.5 mL of RIPA buffer (50 mM tris-HCl, 150 mM NaCl, 1% NP-40, 1 mM EDTA, 1 mM EGTA, 0.1% SDS, 1% sodium deoxycholate, pH 7.5, per 10 mL supplemented with 1 tablet of protease inhibitors and 3 µL benzonase). After incubation with agitation for 1 hr, the lysates were sonicated on ice for 3 min. The lysates were then centrifuged for 20 min at 16 100 rcf at 4 °C and the supernatants were transferred to 2 mL Eppendorf tubes.

For affinity purification a 180 µL bed volume of streptavidin T1 magnetic beads (Invitrogen) was washed in PBS twice and RIPA buffer once before being resuspended in 200 µL RIPA buffer. 90 µL of the beads was added to the forward and reverse samples, respectively. Affinity purification was performed at 4 °C for 3 hr on a rotating wheel.

The beads were carefully washed twice in RIPA buffer and twice in TAP lysis buffer (50 mM HEPES-KOH, 100 mM KCl, 10% glycerol, 2 mM EDTA, 0.1% NP-40, pH 8.0), followed by washing three times in 50 mM ABC to remove all detergents. The beads were resuspended in 200 µL ABC and 10 µL 10 mM DTT (Sigma-Aldrich) in 50 mM ABC was added to reduce disulfide bonds of proteins. After 30 min incubation in a thermomixer at 30 30 °C at 500 rpm, 10 µL 55 mM IAA (Sigma-Aldrich) in 50 mM ABC was added to alkylate the cysteine residues and the samples were incubated in the dark at 30 30 °C at 500 rpm for 30 min. The samples then were digested with 1.5 µg trypsin (Promega) and incubated overnight at 30 30 °C at 1100 rpm. On the next day, the tryptic peptides were separated from beads with a magnetic rack and transferred to fresh 1.5 mL tubes. The digestion was stoped by adding 10 µL 10% TFA and loaded on C18 StageTip columns for purification. After washing with sample buffer (3% TFA, 5% acetonitrile in H_2O) twice, the peptides were eluted from the columns into an autosampler plate with 50 µL buffer B (0,1% formic acid, 80% acetonitrile in H_2O). A vacuum centrifuge (Eppendorf) was used to evaporate the solvent and 8 µL buffer A (5% acetonitrile, 0,1% formic acid in H_2O) was added to the samples.

Peptides were separated on a reverse-phase column on a High Performance Liquid Chromatography (HPLC) system (ThermoScientific) with a gradient set up as the following ratios of buffer B in buffer A: 2 min at 250 µL/min with a linear gradient from 5% to 6% buffer B, 18 min at 200 µL/min with a linear gradient from 6% to 8%, 80 min at 200 µL/min with a linear gradient from 8% to 20%, 80 min at 200 µL/min from 20% to 33%, 20 min at 200 µL/min from 33% to 45%, 2 min at 200 µL/min from 45% to 60%, 1 min at 250 µL/min from 60% to 95%, 5 min at 250 µL/min with 95% buffer B, 1 min at 250 µL/min from 95% to 75%, and 5 min at 250 µL/min at 75% buffer B. Peptides were ionized using an electrospray ionization source (ThermoScientific) and analyzed on a Q-exactive plus Orbitrap instrument (ThermoScientific). The mass spectrometer was operated with Xcalibur in data-dependent acquisition mode with the following parameters: a full MS scan (resolution: 70 000, scan range: 300 to 1700 m/z, AGC target: 1 000 000 ions, maximum injection time: 120 ms) followed by MS-MS analysis (resolution: 17 500, AGC target: 100 000 ions, maximum injection time: 60 ms) on the top 10 abundant ions.

The resulting raw files were analyzed using MaxQuant 1.5.2.8 [18]. The reference human proteome database, consisting of 159 616 entries, was downloaded on February 28th,

2017 from the UniProt Knowledgebase. Lys4, Arg6 and Lys8, Arg10 were added to the labels. Variable modifications were set as N-terminal acetylation and oxidation of methionines. The *in silico* digestion of the reference database was performed with trypsin/P site-specific cleavage. Default global parameters were kept except that "re-quantify" and "match between runs" were turned on. The false discovery rate, assessed by in-parallel searching in a decoy database generated by reversing the reference database, was set at 0.01 at peptide and protein levels. Following analysis was performed using Persius and R 3.3.3.

Transferrin uptake

After 24 hr of doxycycline induction, the cells were starved for 1 hr in serum-free medium supplemented with 20 mM HEPES . Transferrin conjugated with Alexa Fluor 568 (Life Technologies) was diluted in starvation buffer to a final concentration of 10 µg/mL and droplets of 35 µL the transferrin solution were pipetted onto a parafilm in a dark humid chamber. The coverslips were then carefully lifted off the bottom of the plate with forceps and placed face-down on droplets. The humid chamber was incubated at 37 °C and 5% CO_2 for 10 min. After transferrin uptake, the coverslips were washed 3 times for 5 min with PBS supplemented with 10 mM $MgCl_2$ and 10 mM $CaCl_2$, followed by standard immunostaining procedures described below.

Immunostaining and confocal microscopy

Prior to staining, cell culture medium was aspirated and cells were washed with pre-warmed PBS once. The cells were fixed in 4% paraformaldehyde for 15 min at room temperature before being washed 3 times for 5 min in PBS. To permeabilize cells and block unspecific binding sites the cells were incubated for 1 hr at room temperature in blocking buffer consisting of 5% goat serum (Sigma-Aldrich) and 0.3% Triton X-100 (Sigma-Aldrich) in PBS. The primary antibody was diluted in antibody dilution buffer consisting of 1% BSA - Fraction V (Sigma-Aldrich) and 0.3% Triton X-100 in PBS, as indicated in Table 2.3. The coverslips were placed face-down on droplets of 50 µL primary antibody solution on a piece of parafilm in a dark humid chamber. After 1 hr incubation at room temperature, the coverslips were placed face-up in the plate and washed 3 times for 5 min in PBS. Similarly, the coverslips were incubated with secondary antibody solution for 1 hr at room temperature in the humid chamber before being washed for 5 min in PBS. The coverslips were then counterstained with DAPI in PBS for 3 min and washed for 10 min in PBS. Finally, the coverslips were washed briefly with MilliQ H_2O and mounted with ProLong Gold Antifade Mountant (Life Technologies) on slides. After overnight incubation, the slides were stored at 4 °C in

the dark.

TABLE 2.3: Antibodies for immunofluorescence and their dilutions.

Antibodies	**Source**	**Dilution**	**Conjugate**
Mouse monoclonal anti-FLAG	Sigma-Aldrich	1:200	
Rabbit monoclonal anti-EEA1	Cell Signaling Technology	1:100	
Rabbit monoclonal anti-Rab9	Cell Signaling Technology	1:100	
Rabbit monoclonal anti-Rab11	Cell Signaling Technology	1:100	
Rabbit monoclonal anti-LAMP1	Cell Signaling Technology	1:100	
Goat anti-Mouse IgG (H+L)	Invitrogen	1:500	Alexa Fluor 488
Donkey anti-Rabbit IgG (H+L)	Invitrogen	1:500	Alexa Fluor 568

Images in this thesis were acquired using Leica DMI6600 confocal laser scanning microscope with a HCX PL APO 63.0×/1.40 oil objective. As summarized in Table 2.4, fluorophores were excited using 405 nm laser diode, Argon 488 nm laser (20% power) and DPSS 561 nm laser and detected using photomultiplier tubes (PMT). Pinhole diameter was set to 95.6 µm, scanning mode was unidirectional, line average was 2, sampling speed was 400 Hz, and zoom was 5. The voxel size was set to 48.1 nm (width) × 48.1 nm (height) × 125.9 nm (depth).

TABLE 2.4: Settings for fluorescence excitation and detection.

Fluorophore	**Laser line**	**Laser intensity**	**PMT**	**PMT gain**	**PMT offset**
DAPI	405 nm	8.00%	413-477 nm	619 V	-1
Alexa 488	488 nm	12.00%	506-598 nm	646 V	-1
Alexa 568	561 nm	15.00%	580-710 nm	619 V	-1

The z-stack confocal microscopy images were further analyzed using ImageJ 1.51j. The stack viewing and color options were set as the default configuration of the Bio-Formats plugin. One z slice was selected in each image to represent all stacks. The brightness and contrast of the channels were uniformly adjusted in each staining experiment.

Results

3.1 Expression of GLUT1 in stable inducible cell lines

3.2 Proximity labeling of GLUT1 variants

3.3 Subcellular localization study of GLUT1 variants

Discussion

List of Abbreviations

ABC	Ammonium bicarbonate
AGC	Automatic gain control
BSA	Bovine serum albumin
CPZ	Chlorpromazine
CSF	Cerebrospinal fluid
DAPI	4?,6-Diamidino-2-phenylindole
DMEM	Dulbecco's modified Eagle's medium
DPSS	Diode-pumped solid-state
DTT	Dithiothreitol
EDTA	Ethylenediaminetetraacetic acid
GFP	Green fluorescent protein
GLUT1	Facilitated glucose transporter member 1
G1DS	Glucose transporter 1 deficiency syndrome
HEK	Human embryonic kidney
HEPES	4-(2-Hydroxyethyl)-1-piperazineethanesulfonic acid)
HPLC	High-pressure liquid chromatography
HRP	Horseradish peroxidase
IAA	Iodoacemtamide
MS	Mass spectrometry
MS/MS	Tandem mass spectrometry
PBS	Phosphate-buffered saline
PMT	Photomultiplier tube
PVDF	Polyvinylidene fluoride
RIPA	Radioimmunoprecipitation assay
rpm	Revolutions per minute
SDS-PAGE	Sodium dodecyl sulfate polyacrylamide gel electrophoresis
SILAC	Stable isotope labeling by amino acids in cell culture
TAP	Tandem affinity purification

TBST	Tris buffered saline with tween 20
TFA	Trifluoroacetic acid
TGN	Trans-Golgi network
Tris	Tris(hydroxymethyl)aminomethane

Acknowledgements

The acknowledgments and the people to thank go here, don’t forget to include your project advisor…

References

[1] J. M. Pascual, D. Wang, R. Yang, L. Shi, H. Yang, and D. C. De Vivo, "Structural signatures and membrane helix 4 in glut1: inferences from human blood-brain glucose transport mutants," The Journal of Biological Chemistry **283**, 16732–16742 (2008).

[2] M. Mueckler, "Facilitative glucose transporters," European Journal of Biochemistry **219**, 713–725 (1994).

[3] M. Uldry and B. Thorens, "The slc2 family of facilitated hexose and polyol transporters," Pflügers Archiv **447**, 480–489 (2004).

[4] W. L. Lee and A. Klip, "Shuttling glucose across brain microvessels, with a little help from glut1 and amp kinase. focus on 'amp kinase regulation of sugar transport in brain capillary endothelial cells during acute metabolic stress'," American Journal of Physiology - Cell Physiology **303**, C803–C805 (2012).

[5] T. J. Wheeler and P. C. Hinkle, "The glucose transporter of mammalian cells," Annual Review of Physiology **47**, 503–517 (1985).

[6] M. M. M. Paul W. Hruz, "Structural analysis of the glut1 facilitative glucose transporter," Molecular Membrane Biology **18**, 183–193 (2001).

[7] R. Duelli and W. Kuschinsky, "Brain glucose transporters: relationship to local energy demand," Physiology **16**, 71 (2001).

[8] D. C. De Vivo, R. R. Trifiletti, R. I. Jacobson, G. M. Ronen, R. A. Behmand, and S. I. Harik, "Defective glucose transport across the blood-brain barrier as a cause of persistent hypoglycorrhachia, seizures, and developmental delay," New England Journal of Medicine **325**, 703–709 (1991).

[9] J. Klepper, M. Willemsen, A. Verrips, E. Guertsen, R. Herrmann, C. Kutzick, A. Flörcken, and T. Voit, "Autosomal dominant transmission of glut1 deficiency," Human Molecular Genetics **10**, 63–68 (2001).

[10] D. Wang, J. M. Pascual, H. Yang, K. Engelstad, S. Jhung, R. P. Sun, and D. C. De Vivo, "Glut-1 deficiency syndrome: clinical, genetic, and therapeutic aspects." Annals of Neurology **57**, 111–118 (2005).

[11] W. G. Leen, J. Klepper, M. M. Verbeek, M. Leferink, T. Hofste, B. G. van Engelen, R. A. Wevers, T. Arthur, N. Bahi-Buisson, D. Ballhausen, J. Bekhof, P. van Bogaert, I. Carrilho, B. Chabrol, M. P. Champion, J. Coldwell, P. Clayton, E. Donner, A. Evangeliou, F. Ebinger, K. Farrell, R. J. Forsyth, C. G. E. L. de Goede, S. Gross, S. Grunewald, H. Holthausen, S. Jayawant, K. Lachlan, V. Laugel, K. Leppig, M. J. Lim, G. Mancini, A. D. Marina, L. Martorell, J. McMenamin, M. E. C. Meuwissen, H. Mundy, N. O. Nilsson, A. Panzer, B. T. Poll-The, C. Rauscher, C. M. R. Rouselle, I. Sandvig, T. Scheffner, E. Sheridan, N. Simpson, P. Sykora, R. Tomlinson, J. Trounce, D. Webb, B. Weschke, H. Scheffer, and M. A. Willemsen, "Glucose transporter-1 deficiency syndrome: the expanding clinical and genetic spectrum of a treatable disorder," Brain **133**, 655–670 (2010).

[12] A. Suls, P. Dedeken, K. Goffin, H. Van Esch, P. Dupont, D. Cassiman, J. Kempfle, T. V. Wuttke, Y. Weber, H. Lerche, Z. Afawi, W. Vandenberghe, A. D. Korczyn, S. F. Berkovic, D. Ekstein, S. Kivity, P. Ryvlin, L. R. F. Claes, L. Deprez, S. Maljevic, A. Vargas, T. Van Dyck, D. Goossens, J. Del-Favero, K. Van Laere, P. De Jonghe, and W. Van Paesschen, "Paroxysmal exercise-induced dyskinesia and epilepsy is due to mutations in slc2a1, encoding the glucose transporter glut1," Brain **131**, 1831–1844 (2008).

[13] J. Klepper and B. Leiendecker, "Glut1 deficiency syndrome–2007 update," Developmental Medicine and Child Neurology **49**, 707–716 (2007).

[14] L. Slaughter, G. Vartzelis, and T. Arthur, "New glut-1 mutation in a child with treatment-resistant epilepsy," Epilepsy Research **84**, 254–256 (2009).

[15] K. N. Pandey, "Functional roles of short sequence motifs in the endocytosis of membrane receptors," Frontiers in Bioscience (Landmark Ed) **14**, 5339–5360 (2009).

[16] H. Dinkel, K. Van Roey, S. Michael, M. Kumar, B. Uyar, B. Altenberg, V. Milchevskaya, M. Schneider, H. Kühn, A. Behrendt, S. L. Dahl, V. Damerell, S. Diebel, S. Kalman, S. Klein, A. C. Knudsen, C. Mäder, S. Merrill, A. Staudt, V. Thiel, L. Welti, N. E. Davey, F. Diella, and T. J. Gibson, "Elm 2016—data update and new functionality of the eukaryotic linear motif resource," Nucleic Acids Research **44**, D294–D300 (2016).

[17] A. L. Couzens, J. D. R. Knight, M. J. Kean, G. Teo, A. Weiss, W. H. Dunham, Z.-Y. Lin, R. D. Bagshaw, F. Sicheri, T. Pawson, J. L. Wrana, H. Choi, and A.-C. Gingras,

"Protein interaction network of the mammalian hippo pathway reveals mechanisms of kinase-phosphatase interactions," Science Signaling **6**, rs15 (2013).

[18] J. Cox, M. Y. Hein, C. A. Luber, I. Paron, N. Nagaraj, and M. Mann, "Accurate proteome-wide label-free quantification by delayed normalization and maximal peptide ratio extraction, termed MaxLFQ," Molecular & Cellular Proteomics : MCP **13**, 2513–2526 (2014).